Journal of Molecular Liquids 399 (2024) 124481

Contents lists available at ScienceDirect

Journal of Molecular Liquids

journal homepage: www.elsevier.com/locate/molliq

Innovative stearic acid-in-silicone oil (o/o) phase change material lubricating emulsions (PCMLEs): Thermo-rheological and tribological properties

C. Delgado-Sánchez, E Cortés-Triviño, A. Tenorio-Alfonso, F.J. Navarro *

Pro²TecS-Chemical Process and Product Technology Research Centre, Department of Chemical Engineering, ETSI, Campus de "El Carmen", University of Huelva, 21071 Huelva, Spain

ARTICLE INFO

Keywords:
Phase change emulsions
Phase change materials
Lubricants
Wear
Rheology

ABSTRACT

This paper analyses the feasibility of using novel non-aqueous stearic acid-in-silicone oil (o/o) phase change material lubricating emulsions (PCMLEs). The novel use of these dispersions with heat storage capacity for lubricating applications can be considered a new approach since they have not yet been used for such purposes. In this study, PCMLEs consist of stearic acid, with a melting point of roughly 69 °C, as a dispersed phase change material in a continuous silicone oil medium. Samples were prepared by mixing different phase ratios, by high-shear processing and stabilised by a constant concentration of a silicone-based non-ionic surfactant. Taking into consideration the ability of stearic acid to absorb latent thermal energy during machinery operation, the potential application in lubrication has been assessed by means of stationary and temperature ramp friction tests. Moreover, the effect of the phase transition on the PCMLEs' rheological response has been analysed through stationary flow tests and frequency sweeps within the linear viscoelastic range at constant temperatures, below (40 °C) and above (80 °C) the melting process of the disperse phase. Additionally, their thermal properties and morphology were also studied through X-ray diffraction measurements (XRD), differential scanning calorimetry (DSC) and polarised optical microscopy. As a result, the reported rheological properties and microstructure led to the enhancement in tribological characteristics of PCMLEs since a significant reduction in the friction factor is evidenced, within the whole temperature range, when compared to the silicone oil.

1. Introduction

In recent years, there has been an increased emphasis on developing high-performance lubricants that can improve the efficiency and longevity of machines and equipment. Awareness of the critical importance of the use of lubricants in today's world is growing in the metalwork industry, especially in high-temperature applications such as in engines, turbines, bearings and other machinery that operate in extreme heat conditions where their life cycle is being undermined as a consequence of the generated friction and wear [1].

The choice of lubricant depends on the specific application, as well as factors such as operating conditions, temperature, pressure, and load. Thus, the use of mineral oils, one of the most commonly used lubricants on the market [2] entails disadvantages in terms of preserving their properties for sufficient periods, which, together with the low affinity with metal surfaces due to their non-polar characteristics [3], leads the lubricant community to look for enhanced formulations that allow the life cycle of machinery to be extended. For instance, in high-speed rolling processes, the temperature can easily reach 200 °C due to the high forming pressure [3], seriously affecting those oil-based lubricants' properties due to their oxidation and the protective film rupture in metal contacts.

Within the lubricants used in metalworking, oil-in-water (o/w) emulsions have been reported to have good properties helping to improve tool life and workpiece quality [4,5]. They show an important compromise between the droplets' stability inside the emulsion, the ability to form a protective tribo-film, and the permanent supply to the contact area, which is required to get good tribological properties reducing friction and wear [6,7]. In this sense, o/w emulsions based on highly polar vegetable oils have been proposed by some authors trying to solve the compatibility issues with metal surfaces in these applications, providing better cooling and lubrication compared to pure oils,

* Corresponding author.
E-mail address: frando@uhu.es (F.J. Navarro).

https://doi.org/10.1016/j.molliq.2024.124481
Received 12 February 2024; Received in revised form 11 March 2024; Accepted 12 March 2024
Available online 14 March 2024

which can be beneficial for high-speed machining operations [8,9]. However, those vegetable oils-based emulsions may also have some drawbacks compared to other lubricants, such as some derived problems related to the generated carbon residues during the process that could make cleanliness difficult or affect the surface accuracy of the machined part [10]. Moreover, although these emulsions show a high surface affinity due to their polar components, they also present microbial growth and a limited range of temperatures in which they can effectively operate in stable conditions [11,12]. Understanding the tribology and rheology of emulsions at high temperatures is of principal importance to the application of the emulsions. Thus, some emulsion formulations have been used in high-temperature applications to provide not only lubrication but also cooling, through complex and not very well-known destabilisation and evaporation mechanisms of the aqueous phase [13].

Accordingly, the development of advanced lubricants, improving compatibility with metal, operating stably over a broad range of temperatures, as well as in humid and oxidising conditions, remains challenging. To solve these issues, oil-in-oil (o/o) emulsions could be an interesting option to explore in this field. This kind of emulsion is widely used in cosmetics and pharmaceuticals but their applications in lubrication are practically unknown, as there are only a few patents [14].

The use of phase change materials (PCMs) in lubrication is another emerging area of research that shows promise for improving the performance and efficiency of lubricants in various applications [15,16]. PCMs are materials that can store and release thermal energy by undergoing a phase transition, typically from a solid to a liquid state, at a specific temperature [17]. In lubrication, PCMs can be especially beneficial in high-temperature applications, where overheating can cause premature wear and damage to the machine as they can be used to absorb excess heat and maintain a more stable operating temperature, which can improve the overall performance and reliability of the system. To the best of our knowledge, there are only a few studies investigating the development of novel lubricant formulations that incorporate PCMs and those studies are extremely recent. They incorporate PCM to form composites, either by injecting it directly into a porous matrix [18] or through the incorporation of microcapsules into an elastomeric matrix [15], but none of them use emulsion-based technologies.

Therefore, the incorporation of PCM, as the disperse phase, to formulate the so-called phase change material lubricating emulsions (PCMLE), would allow to open the path to a new approach for lubricating applications. Then, PCMLEs will combine the advantages of o/o emulsions such as thermal and chemical stability, at high temperatures, with improved heat storage capacity of the PCM, better heat transfer rate associated with the larger specific surface area and adequate pumpability [19]. In general, non-aqueous phase change material emulsions have only recently been investigated by the authors for their use in energy storage applications [20] and, as far as we know, it has never before been studied for lubrication purposes.

In a very recent study [21], despite the lack of information regarding that kind of emulsions, the authors successfully reported a fully stable PCM dispersion, stearic acid-in-silicone oil emulsion, with potential as a lubricant for high-temperature applications, together with the capability of storing and releasing thermal energy. In particular, silicon oil-based lubricants have been previously reported as thermally stable materials, more specially polydimethylsiloxane (PDMS) silicone oil has proven to be an excellent alternative as an external lubricant coating in stainless-steel contacts with outstanding tribological characteristics, at high shear rates [22]. Moreover, the use of stearic acid as the dispersed phase of the emulsion is also advantageous since, as saturated fatty acid, it has been previously employed as a significant lubricating additive to reduce wear and friction in tribological contact [23]. Thus, in addition to the improvement in chemical compatibility with metal surfaces, the phase change process of the dispersed phase, at 69 °C, would help to decrease the surface temperature of a bearing, improving its performance and reducing the risk of failure.

Therefore, the focus of this research was the thermorheological and tribological assessment of novel PCMLE in pursuit of feasible lubricating material. For that purpose, PCMLEs bearing different proportions of dispersed stearic acid were subjected to a comprehensive characterisation, comprising tribological stationary and temperature ramps, rheological flow tests and small amplitude oscillatory shear analysis, as well as thermal, microstructural and morphological evaluation.

2. Materials and methods

2.1. Materials

Oil-based phase change material lubricating emulsions (PCMLEs) encompass phase change material's (stearic acid) droplets dispersed in a continuous oily phase (silicone oil) by using a selected stabilizer (surfactant). Thus, stearic acid (SA), whose melting temperature is centred at 69 °C, provided by Sigma-Aldrich (Spain) forms the disperse phase. A selected industrial low-viscosity silicone oil, ESQUIM FH-100 (polydimethylsiloxane - PDMS, viscosity 0.1 Pa·s at 25 °C) was supplied by Esquim S.A. (Spain) and regarded as the continuous phase. PCMLEs were stabilized by a silicone-based non-ionic surfactant, ABIL Care XL80 (Bis-PEG/PPG-20/5 PEG/PPG-20/5 Dimethicone (and) Methoxy PEG/PPG-25/4 Dimethicone (and) Caprylic/Capric Triglyceride; HLB calculated = 11), which was purchased from Evonik Nutrition & Care GmbH (Germany).

2.2. Sample preparation

PCMLEs were prepared following the emulsification process previously detailed in [21]. In brief, all compounds were firstly preconditioned at 80 °C, aimed at ensuring the liquid state of stearic acid. Afterwards, the surfactant was dissolved in silicone oil, with the subsequent dropwise addition of molten stearic acid, according to the proportions established in Table 1. These mixtures were subjected to simultaneous homogenisation under high shear conditions (20000 rpm) by using an Ultra-Turrax T25 homogeniser (IKA, Germany).

2.3. Methods

2.3.1. Rheological characterisation

The rheological response of the developed PCMLEs was studied at the temperatures of 40 and 80 °C, below and above the crystallisation/melting points of the stearic acid. First, rotational viscous flow analyses were conducted within the shear rate range from 0.01 up to 100 s^{-1}, using a controlled-strain Ares-G2 rheometer (TA Instruments, USA), fitted with a smooth Couette geometry (cup diameter of 30 mm, bob diameter of 27 mm, bob length of 42 mm), with an operating gap of 2 mm and a Peltier temperature control system. Small Amplitude Oscillatory Shear (SAOS) tests were also carried out at 40 °C, in a controlled-stress rheometer Physica MCR 501 (Anton Paar, Graz, Austria), between the frequency range from 0.03 to 100 rad·s^{-1}, using a plate-plate geometry (50 mm diameter, 1 mm gap) within the Linear Viscoelastic Region (LVR) evaluated in previous Stress Sweep experiments conducted at 1 Hz.

2.3.2. X-ray diffraction measurements (XRD)

The crystalline structure of pure stearic acid and the PCMLE were

Table 1
Compositions of PCMLEs.

Sample	Weight ratio of Silicone Oil to Stearic acid	Silicone Oil (wt.%)	Stearic acid (wt.%)	Surfactant (wt.%)
SA10	90/10 = 9	89.11	9.90	0.99
SA5	95/5 = 19	94.53	4.98	0.49
SA1	99/1 = 99	98.90	1.00	0.10

analysed using a D8 Advance X-ray diffractometer (Bruker-AXS, Germany) at room temperature (25 °C). The X-ray diffraction pattern was obtained under the following instrumental conditions: 30 mA, 40 kV, angle 2θ: 4° and 59.9°, step size = 0.019°. A copper Kα/K target (λ = 1.54) was used for the generation of the X-rays. All the samples were prepared by placing a small amount on a supporting glass slide of 25 × 25 mm^2, which was heated over stearic acid melting temperature (80 °C) to flatten and obtain approximately 1 mm-thick film followed by cooling to room temperature. Afterwards, the sample-containing slide was located at the centre of a metal holder, externally shaped to be allocated in the instrument.

2.3.3. Differential scanning calorimetry (DSC)

The thermal properties of the anhydrous PCMLEs were evaluated in a differential scanning calorimeter DSC250 (TA Instruments, USA). Hermetic aluminium pans, loaded with 5–10 mg of emulsion, were heated up to 30 °C and subsequently submitted to a double heating–cooling cycle from 30 to 80 °C, with a scan rate of 1 °C·min^{-1}, under inert purge of nitrogen (50 mL·min^{-1}). All thermal events, mainly melting and crystallisation processes were identified and characterized from the resulting thermograms. Therefore, the following parameters were estimated: the crystallisation/melting onset-temperatures (T_c^{onset}, T_m^{onset}) were obtained from the intersection point of the extrapolated baseline and the inflectional tangent at the beginning of the crystallisation/melting peaks from the cooling/heating scans; the crystallisation/melting peak-temperatures (T_c^{peak}, T_m^{peak}) was regarded as the temperature ascribed to the largest deviation of the heat flow signal from the virtual baseline; the crystallisation/melting enthalpies (ΔH_c, ΔH_m) were determined by the numerical integration of the area enclosed within the crystallisation/melting peaks.

2.3.4. Tribological characterisation

Tribological properties of the formulated PCMLE were evaluated in a Physica MCR 501 controlled-stress rheometer (Anton Paar, Graz, Austria) coupled with a ball-on-three-plates tribological cell [24]. The experimental setup comprises a lower measuring geometry with three 45°-inclined steel plates (1.4301 AISI 304, 0.21 μm roughness, 80 HRB hardness) where the PCMLEs were placed, together with an upper measuring geometry fitted with a fixed 6.35 mm-radious bearing ball (1.4401 grade 100 AISI 316). Such ball-on-three-plates configuration enables the friction coefficient (f) determination as the ratio between the applied normal force (F_N) and the measured friction force (F_F) (see Equation (1).

$$f = \frac{F_F}{F_N} \tag{1}$$

Therefore, the stationary friction coefficient of all formulated emulsions on steel-steel contact was evaluated over time at constant temperatures (40 and 80 °C), under 20 N of F_N and at the rotational speed of 10 rpm. Such sliding velocity was selected to compare the stationary friction coefficients of the different emulsions under the same test conditions. Additionally, tribological heating and cooling temperature ramps from 40 to 100 °C and the other way around, were also performed by applying 20 N of F_N and 1 °C·min^{-1} of heating/cooling rate. At least five replicates of each tribological experiment were carried out on fresh samples, establishing a duration of measurement per point of 120 s to ensure stationary friction values.

2.3.5. Optical microscopy

An Olympus System Microscope BX52 (Japan) fitted with a light polarizer and an Olympus Digital Camera C5050Z with an objective of 4x were used to analyse the morphology of the prepared PCMLE before and after the previously detailed tribological temperature ramps tests at room temperature. However, due to the abrasive wear mechanism obtained after friction tests on steel-steel contact, this morphological characterisation was carried out after performing the tribological temperature ramps tests on PMMA-steel contact. Thus, the lower measuring geometry with three 45°-inclined steel plates was replaced by PMMA plates with similar characteristics to the former to prevent metal wear and the subsequent presence of metallic particles in the formulations. After tribological measurements, PCMLEs were carefully poured into the sample holder (76 × 26 mm), obtaining the optical images under ordinary and cross-polarized light.

Additionally, evaluation of the friction tracks remaining on the steel plates upon conducting stationary tribological experiments at both temperatures (40 and 80 °C) was also conducted by using optical microscopy at 4x magnification. The ensuing track values are reported as the average resulting from the three steel plates after running six replicates.

3. Results and discussion

3.1. Crystalline structure of the disperse phase

The knowledge of the crystalline structure of dispersions is of paramount importance for the proposed application, because it is directly related to the energy storage capacity since a large crystallinity will lead to a high phase change enthalpy [25]. In this sense, Fig. 1 shows the wide-angle XRD patterns of pure stearic acid (Fig. 1A) and stearic acid-in-silicone oil emulsions (Fig. 1B), which provides information about the crystal morphology of the samples.

For pure stearic acid (Fig. 1A), the XRD pattern is characterised by the presence of several well-defined peaks, where those placed at 2Θ = 21.6° and 24.0° are attributed to interplanar spacings of ordered molecules, pointing out its crystalline state [26,27]. Therefore, the melting and crystallization of stearic acid crystals, presented in DSC

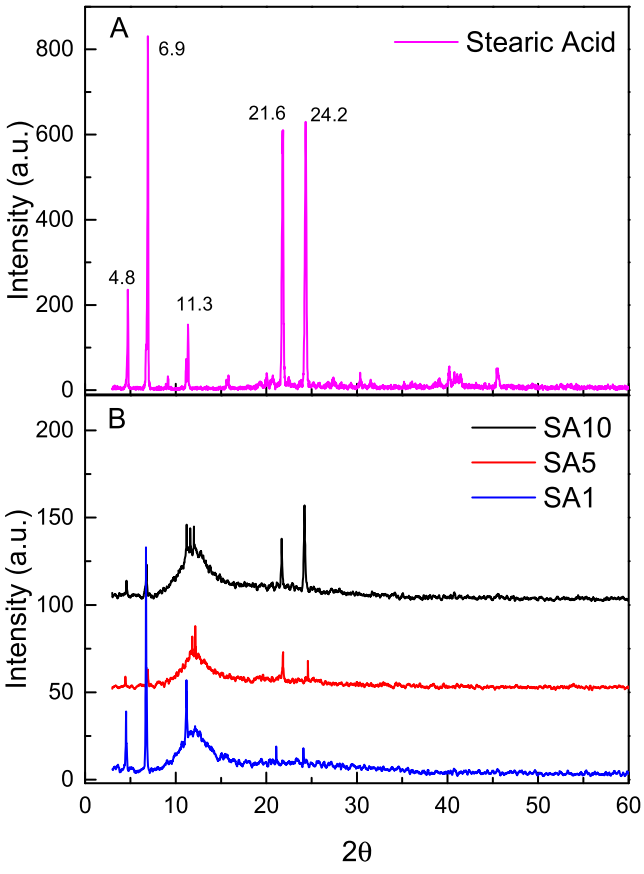

Fig. 1. XRD patterns of a) pure stearic acid and b) non-aqueous phase change material lubricating emulsions (PCMLEs).

thermograms (Fig. 2), are responsible for the thermal energy storage and release during heating and cooling.

Concerning PCMLEs, on the one hand, XRD spectra display a large diffraction halo at around 12° (Fig. 1B) which is ascribed to the continuous silicone oil phase of the emulsion, since similar profiles have been reported for amorphous polydimethylsiloxane elsewhere [28,29]. On the other hand, for all PCMLEs, the same conspicuous diffraction peaks attributed to the stearic acid can be noticed as well, but with intensities proportional to the disperse phase ratio. Particularly, the mentioned maxima corresponding to the interplanar spacing of stearic acid (21.6° and 24.0°), were not shifted with concentration, a fact that points out that the stearic acid exists in its crystalline form in all emulsions, even for the least concentrated one, at room temperature. These results also indicated that the internal crystal structure of stearic acid was not affected during the emulsification process [30].

This is consistent with the results obtained in the DSC measurements (Fig. 2 and Table 2) where it can be observed that the normalised enthalpies of the stearic acid, in the emulsion were practically unaffected and hence the total crystallinity. However, Fig. 2 and Table 2 point out a clear decrease of phase change temperatures (T_m^{peak} and T_c^{peak}) when disperse phase concentration does, a fact that reveals partial compatibility of crystal structures of stearic acid with silicone oil and surfactant. Therefore, even though stearic acid crystal spacing is unaltered after emulsification i.e. disperse phase presents similar nano-scale morphology, this outcome is usually attributed to the partial disruption of the micro-crystalline structure, as a consequence of the high shear processing, which led to smaller size of crystals formed [21].

It is worth mentioning that, according to DSC results, solid stearic acid crystals are present after cooling emulsions, below the phase change interval and, therefore, led to the development of a suspension of solid structures. By contrast, above the melting interval, liquid melted droplets dispersed in the silicone phase would form a genuine emulsion. Therefore, although the concept of phase change material emulsion is extensively accepted, and so used along this paper, strictly speaking, it would be more appropriate to use a more generic term as dispersions of PCM.

3.2. Rheological behaviour

Formulated PCMLEs were characterised under Small Amplitude Oscillatory Shear (SAOS) conditions at 40 °C, below the crystallization temperature of the disperse phase. Fig. 3 collects the resulting complex modulus (G*) and loss tangent (tan δ = G''/G') as a function of applied frequency. According to this figure, under these conditions, all stearic acid-based dispersions exhibited a gel-like behaviour, typically

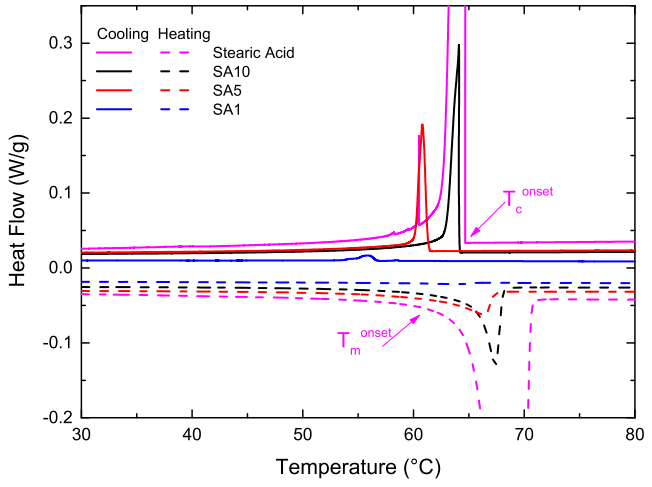

Fig. 2. Heating and cooling DSC scans at 1 °C·min^{-1}, for pure stearic acid and PCMLEs.

Table 2
Physicothermal properties of stearic acid and PCMLEs after applying tribo-temperature tests.

CRYSTALLIZATION					
DSC					Friction curves *
Sample	T_c^{onset} (°C)	T_c^{peak} (°C)	ΔH_c (J/g)	ΔH_c (J/g SA)	T_c^{frict} (°C)
Stearic Acid	64.6	64.7	225.2	225.2	–
SA10	64.1	64.1	21.2	213.8	72.7
SA5	61.3	60.8	10.4	208.6	69.6
SA1	56.6	55.9	1.8	180.2	51.1

MELTING					
DSC					Friction curves *
Sample	T_m^{onset} (°C)	T_m^{peak} (°C)	ΔH_m (J/g)	ΔH_m (J/g SA)	T_m^{frict} (°C)
Stearic Acid	67.1	68.6	223.2	223.2	–
SA10	65.7	67.4	22.0	221.9	52.2
SA5	61.3	66.3	10.5	210.6	59.3
SA1	55.0	63.8	1.1	112.1	54.0

* T_m^{frict} and T_c^{frict} were calculated from tribo-temperature curves (Fig. 9).

characterised by a predominant elastic response (tan δ < 1) and a minimum value of loss tangent (see Fig. 3B), while complex moduli showed an almost negligible reliance on the frequency magnitude.

However, as previously reported [21], both linear viscoelastic responses and gel stiffness are strongly concentration-dependent. This effect is especially remarkable when rising the disperse phase content from roughly 1 up to 5 wt%, since it led to a significant increase in G^* values from 57 Pa up to $3.5{\cdot}10^5$ Pa (at 1 rad·s^{-1}) and, therefore, to gels with a more structured supramolecular network. Further the addition of stearic acid, from 5 to 10 wt%, imparted the PCMLE with a stronger gel-like structure, at 40 °C, with larger G* values and a clear loss tangent minimum (see Fig. 3B). This rheological behaviour is a consequence of the development of a three-dimensional network of crystallised stearic acid particles which are physically interconnected with each other [21]. By contrast, at low stearic acid content (SA1), a much weaker structured network is revealed by its viscoelastic response, with the lowest G* values and the presence of a shoulder in loss tangent rather than a minimum [31].

The flow behaviour of the PCMLEs was also evaluated under steady-state conditions at 40 and 80 °C, i.e., below and above the phase change of the stearic acid. Fig. 4 displays the ensuing steady-state flow curves for all the stearic acid-based dispersions, i.e., the apparent viscosity (η) versus shear rate ($\dot{\gamma}$). As expected, stationary viscosity values of PCMLEs, at 40 °C, are very sensitive to the disperse phase concentration, as in the case of SAOS measurements. In addition, is noteworthy that the melting of the continuous phase (see 80 °C curves in Fig. 4) dramatically modified the rheological response. Then, at 40 °C, regardless of the dispersed phase content, a sharp non-Newtonian behaviour can be observed, while a Newtonian response, with similar values among samples, is evidenced at 80 °C upon melting of the stearic acid [21]. As an example, in the case of dispersion SA10 the apparent viscosity recorded at 1 s^{-1} decreased from around 133.44 up to 0.032 Pa·s when heating to 80 °C (see Fig. 4).

Additionally, the applicability of the empirical Cox-Merz rule (see Equation (2) was also analysed, according to which oscillatory complex (η^*) and apparent (η) viscosities can be superimposed at equivalent frequency (0.01–100 rad·s^{-1}) and shear rate (0.01–100 s^{-1}) values, i.e., $\dot{\gamma} = \omega$ [32,33], which is particularly useful to overcome the occurrence of likely experimental limitations [32,34].

$$\eta(\dot{\gamma}) = \eta^*(\omega) \quad (2)$$

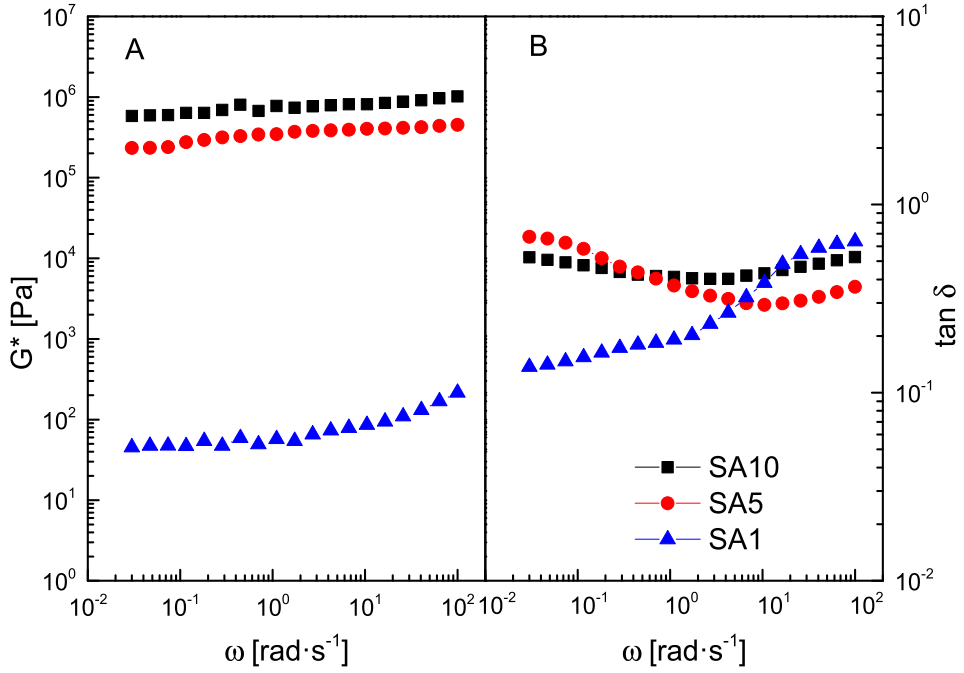

Fig. 3. SAOS analysis results for all PCMLEs at 40 °C as a function of frequency, including a) complex modulus (G*) and b) loss tangent (tan δ).

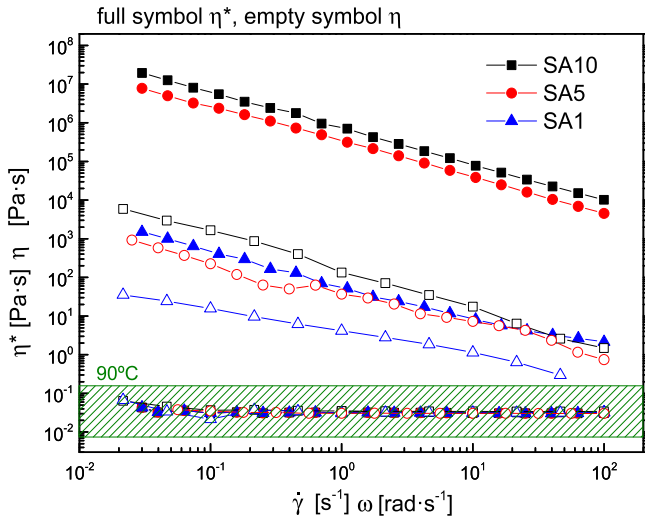

Fig. 4. Complex viscosity (η*), at 40 °C, and steady-state apparent viscosity (η), at 40 and 80 °C, for the formulated phase change emulsions.

As can be deduced from Fig. 4, at 40 °C, the pseudoplastic behaviour of the stearic acid-based dispersions was also observed under SAOS conditions. However, the complex viscosity remained markedly superior to the steady-state counterpart, within the whole experimental range. As established in previous studies [34–37], such departure from the conventional Cox–Merz rule might be ascribed to the disruption of the microstructure as a consequence of the severe strain magnitude during the steady-state experiment, against small amplitude considered in the frequency sweeps, typically conducted in the pre-yield region. Furthermore, the magnitude of the deviation appeared to be more remarkable when raising stearic acid content above 1 wt%, which is related to the mentioned development of a network of interacting particles [38]. In this concentration range, the much higher values of complex viscosities compared to steady-shear ones is a typical response of weak-gel networks which can withstand small oscillatory deformations but rupture under higher shear deformation in flow tests.

Consequently, to correlate both apparent and complex viscosities, which have been plotted in Fig. 5, the generalized Cox-Merz rule has been considered in this study [34,37,38].

$$\eta^* = C \cdot \eta^{\alpha} \tag{3}$$

where C and α are experimental parameters, which are gathered in Table 3. According to the results, despite the inadequacy of the conventional Cox-Merz model for the considered PCMLEs, the introduction of the shift factor C and the power index α allowed to provide a proper correlation between both viscosities, for the evaluated PCM suspensions with a disperse phase content ranging from 1 up to 10 wt%, which can be confirmed by the appropriate regression coefficients ($R^2 = 0.99$).

On the other hand, the fitting parameter C is only slightly increased when raising the stearic acid proportion above 5 wt%, while experiencing a dramatic drop of around 99.9 % below that critical concentration (see Table 3), thereby evincing the significantly higher structured network developed in SA10 and SA5, at 40 °C. Similarly, α presented values close to 1, at the higher disperse phase content, while

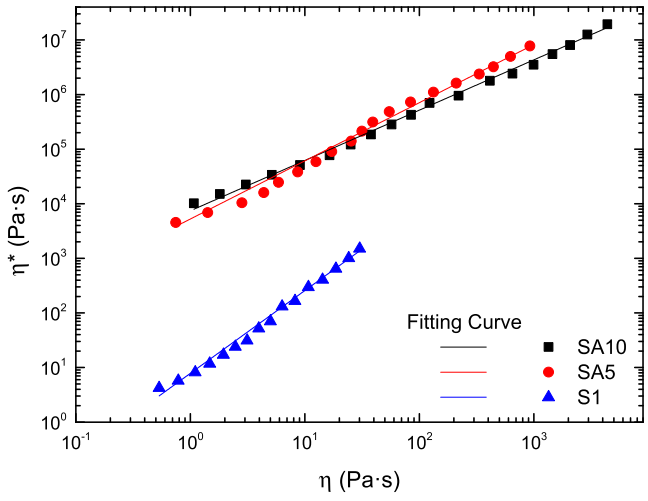

Fig. 5. Correlation between complex (η*) and apparent (η) viscosities, at 40 °C.

Table 3
Generalized Cox-Merz fitting parameters for the studied PCMLEs.

PCMLE	C	α	R^2
SA10	7429.57 ± 212.76	0.92 ± 0.01	0.99
SA5	5250.12 ± 670.76	1.07 ± 0.02	0.99
SA1	7.82 ± 0.19	1.52 ± 0.01	0.99

increasing around 70 % for lower disperse phase concentrations, therefore, revealing the higher susceptibility of its η* to the corresponding steady-state properties.

Consequently, values of the empirical parameters from the generalised Cox-Merz model can therefore be used to estimate steady shear properties from small amplitude oscillatory shear measurements for all PCMLEs at 40 °C.

3.3. Tribological and thermo-physical properties

Fig. 6 shows the stationary friction coefficient curves of all PCMLEs when subjected to a constant normal force of 20 N and a rotational speed of 10 rpm for 10 min. In this study, two different temperatures (40 and 80 °C) were applied while testing to evaluate the tribological behaviour of these emulsions, upon crystallisation of the dispersed phase and in its molten state. As previously established, silicone oil by itself usually exhibits poor tribological characteristics, with relatively high friction coefficients in comparison with other lubricating oils [39,40].

Interestingly, as can be deduced from Fig. 6, a significant reduction in friction coefficients was appreciated when using PCMLEs in tribological contact at both temperatures. Therefore, an improvement of the tribological characteristics was obtained when dispersing stearic acid in this oil, resulting in a remarkable drop in the friction coefficients together with the energy storage capabilities [41]. In general terms, it should be noted that a temperature rise from 40 to 80 °C, led to a significant decrease in the friction coefficients. This outcome is attributed to the melting of the crystallized stearic acid (solid dispersions) that gave rise to the appearance of liquid droplets in emulsions at 80 °C.

In addition, some differences in the friction values can be noticed when modifying the amount of stearic acid used to formulate them. As can be expected, the friction coefficients should be decreased as the viscosity of emulsions increases since a thickened formulation would lead to higher hydrodynamic pressures, thus promoting the entrainments of droplets into the tribological contact [42]. However, for the measurements performed at 80 °C, the values of the friction coefficients were reduced with stearic acid concentration but no differences in viscosity were detected (Fig. 4). In those systems, at 80 °C, the disperse phase remains in its molten state, favouring a non-flocculated dispersion of spherical droplets within the continuous phase, where the relatively low volume fraction of stearic acid does not modify the emulsion flow characteristics [21]. This indicates that the tribological behaviour is not only affected by the viscous properties of materials but also by the emulsion microstructure. On the one hand, taking into account that the liquid stearic acid, at 80 °C, presents the lowest friction coefficient, an increase of the disperse phase concentration of the emulsion is expected to progressively improve the lubricity, as it has been reported for water-based emulsions [43,44]. On the other hand, the droplet size of the disperse phase of the emulsion exerts a notable influence on friction and wear. In this sense, as pointed out by Wang et al. [42], larger droplet sizes could decrease friction as a consequence of the greater ease of being squeezed and entrained into the tribological contact, inducing coalescence and forming the protective friction film more easily. Therefore, the lowest emulsion friction values (0.08) were obtained for those PCMLEs containing a 10 wt% of disperse phase with a diameter of droplets of 6.58 μm [21], where the protective film is more quickly generated, hence diminishing friction. Conversely, a lower concentration resulted in smaller droplet diameters (3.41 μm), as in the SA1 system, generating higher friction in the tribological contact (friction values of 0.15).

Nonetheless, at 40 °C, i.e., at temperatures below its crystallization point, a different trend in the friction behaviour was identified, despite the low friction coefficients obtained. In this case, as it has been previously mentioned, stearic acid remains crystalline leading to a gel-like behaviour and a significant increase in the viscosity of the system (Fig. 4). Thus, an increase in the amount of stearic acid gives rise to a decrease in the friction coefficients, which is in accordance with the rise of emulsion viscosity at 40 °C. Such crystalline structure brings about a major effect on viscosity for the most concentrated emulsions (SA10 and SA5). Thus, lower friction values were obtained for SA10 formulation (0.16) than those shown by suspensions comprising 5 wt% of disperse phase in its crystalline state (0.19 for SA5) due to the formation of stronger microstructural networks. Moreover, stearic acid provides a high affinity to metal surfaces due to the existence of polar components in its chemical structure, which favours adherence to tribological contact. Thereby, a thicker tribo-film would be formed with higher weight fractions of stearic acid, providing a higher separation between the tribological contact and obtaining a uniform decrease in the friction coefficient [10,23]. An unusual behaviour was displayed for SA1, which showed the lowest friction value (0.14) despite containing a smaller amount of crystalline phase. However, the markedly different rheological properties and microstructure could produce a different hydrodynamic lubrication regime, which may make it not directly comparable to the others. Then, the much lower number of crystals in the SA1 emulsion, coupled with the friction-generated heat in a tribological contact, would explain this decrease in the friction coefficients.

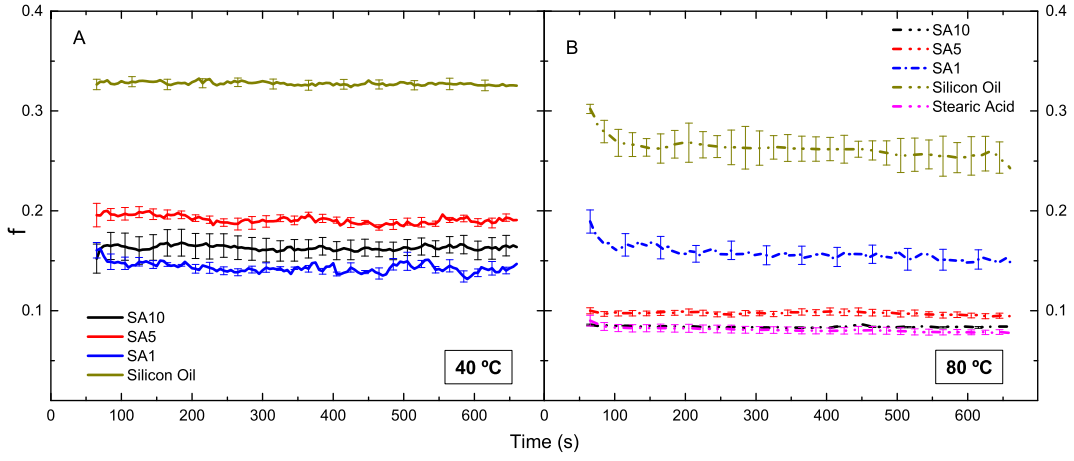

Fig. 6. Stationary friction coefficients (f) of all formulated emulsions at a) 40 °C and b) 80 °C.

Concerning the wear of the metal surfaces, Fig. 7 shows the scar diameters obtained after performing the stationary friction tests under constant load and sliding speed for 10 min. This wear is plotted as a function of the concentration of the disperse phase, comprising the phase change emulsions at two different temperatures (40 and 80 °C). For tests carried out at a low temperature, the existence of solid particles in the oil suspensions could lead to an increase in wear, in comparison with those shown by pure silicone oil, as a consequence of particle sliding during shear [45,46]. However, raising the concentration of stearic acid fosters the achievement of a more structured supramolecular network and an increase in the tribo-film viscosity [21], which, together with the greater number of polar groups and their affinity to metal surfaces, allows for reduced wear [10]. However, as well as the friction coefficients, SA1 formulation resulted in lower wear scar diameter values, probably due to lower concentration of the disperse phase. Despite this, SA1 formulation displayed noticeable differences in wear surface in comparison with the samples comprising higher amounts of stearic acid. As can be seen in Fig. 8, although all formulated dispersions exhibited abrasion characteristics, a lower wear diameter but with wide furrows and dark grooves with deep craters were obtained for suspension containing the lower amount of crystalline phase. In this case, metal particles dispersed freely into emulsion can easily get into the contact zone contributing to wear and generating abrasions [47,48].

Likewise, at high temperature, the wear scar diameters were reduced as the amount in the disperse phase concentration increased. In these formulations, although the viscosity of samples was quite similar to those found by the pure silicone oil at this temperature (80 °C) [21], the wear diameters decreased as a consequence of the easy formation of the wear-protective tribo-film [42]. Thus, larger droplets inducing coalescence and squeezing and entraining into the lubricant contact were obtained when adding a concentration of dispersed phase higher than 5 wt%, easily generating a tribo-film that covers the metal surfaces and provides a noticeable decrease in wear.

On the contrary, SA1 formulation showed a high wear scar diameter, even larger than that shown by the continuous phase, which can be attributed to the relatively low amount of stearic acid forming the non-flocculated dispersion. In this case, the smaller size droplets, which would need extra time to form the wear-protective tribo-film, produced relatively high friction at 80 °C (see Fig. 6), causing abrasion wear on the metal surface and squeezing out metal particles from the contact zone. These expelled particles could accumulate around the edge of the wear scar as a consequence of the low viscosity of the systems, thus enlarging the scar diameter [48]. Finally, the PCMLE comprising the highest concentration (10 wt%) of crystalline phase showed the lowest wear scar diameter, also displaying a smoother wear surface with softer abrasion as a result of the fast formation of the protective film adhered to the tribological contact.

Additionally, the effect of the phase change process and the recovery capacity of these formulations during friction were studied by applying tribological tests under heating and cooling temperature ramps in the 40–100 °C range and compared with DSC scans both performed at 1 °C·min^{-1}. Fig. 9 shows the friction coefficients of the different PCMLEs and their base components when applying 20 N of F_N, 10 rpm of velocity and 1 °C·min^{-1} of heating/cooling rate. Moreover, although the Stribeck curves have not been described in this work, a rough estimation of the Sommerfeld parameter [49] could be obtained by fixing normal load and sliding velocity during the test. Therefore, taking into account that stationary friction values were obtained under these constant conditions, the frictional behaviour of these materials could be analysed as a function of both the viscous properties of each formulation and the prevailing lubrication regime [50]. In general terms, as determined in stationary friction tests, friction coefficients of PCMLEs were notably lower than those obtained by the pure silicone oil in the whole range of temperatures studied. Moreover, these values were drastically reduced as temperature raised, and vice versa, which could be related to two simultaneous phenomena, i.e., the melting/crystallisation of the dispersed phase with modifying temperature and the shifting throughout the different regimes of the Stribeck curve. In addition, as previously mentioned, rheological data pointed out a clear dependence of viscosity on the melting and crystallisation point of the stearic acid [21]. In this way, relatively high friction values were obtained for all systems when applying low temperatures, which match with the melting/crystallisation point of stearic acid obtained in DSC tests (Table 2), providing a higher value of Sommerfeld parameter due to the higher viscosity of these formulations at low temperatures. In this case, the Boundary regime could be dominant in these temperature ranges, since relatively constant friction values were attained. However, as the temperature increased and the sliding was maintained, the stearic acid on the contact surface melted due to the effect of friction heat and temperature increase, which resulted in lower friction coefficients. This is strongly influenced by the viscosity drop of several orders of magnitude that probably yields the shift to the mixed lubrication regime where the friction coefficient is reduced [51]. Nonetheless, although the friction coefficient was variable throughout the temperature range studied, it is noteworthy that after the heating and cooling cycles, the systems were able to recover their tribological properties upon their phase change, thus indicating great stability from the point of view of their friction characteristics.

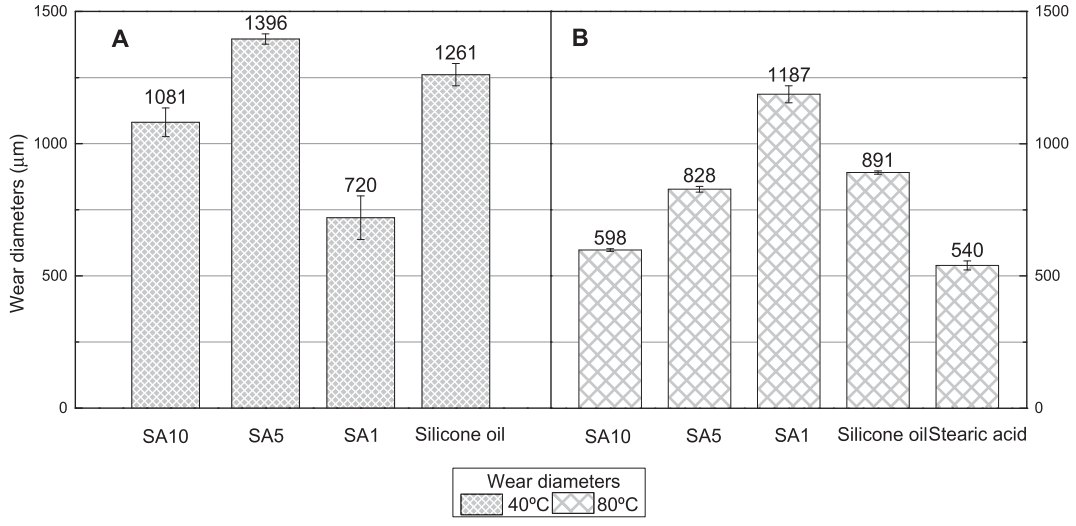

Fig. 7. Wear scar diameters obtained after tribological tests conducted at a different temperature, taken from Fig. 8: a) 40 and b) 80 °C.

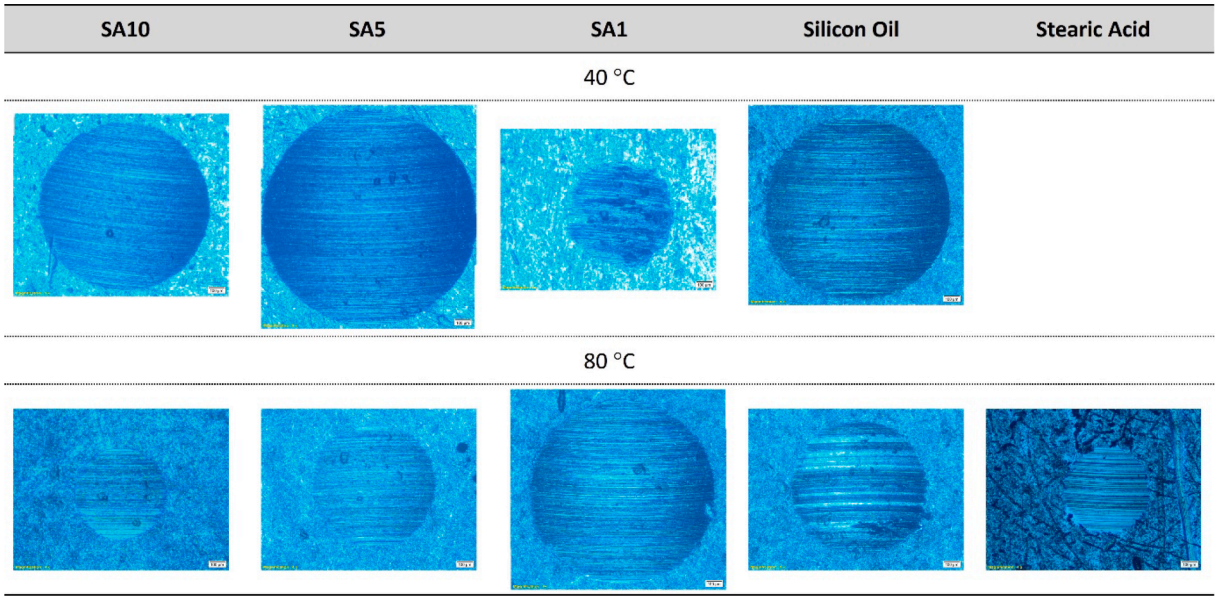

Fig. 8. Wear scar images obtained by optical microscopy after tribological tests.

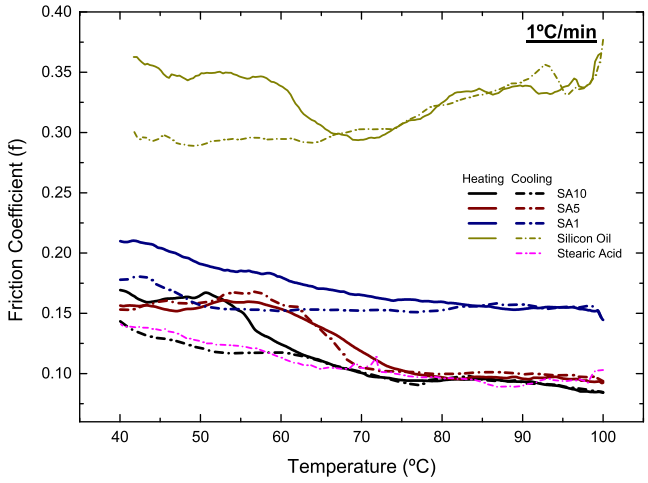

Fig. 9. Friction coefficients (f) of the different PCMLEs and their base components when applying tribological tests under heating and cooling temperature ramps.

Regarding the effect of disperse phase concentration, several differences can be also detected in the tribological curves. As previously stated, thermal characterisation was conducted on fresh PCMLEs and the effect of friction over the onset of melting (T_m^{onset}) and crystallisation (T_c^{onset}) points, and their corresponding enthalpies (ΔH_m, ΔH_c) is the subject matter of this study. Consequently, as can be seen from the thermal results collected in Table 2, the peak and onset melting and crystallisation temperatures (Fig. 2), as well as their corresponding enthalpies have been calculated from DSC tests.

Furthermore, it is important to note that, a more pronounced shift in both phase change temperatures (from 9 to 12 °C), was appreciated in tribological temperature ramps in comparison with DSC data i.e. without shearing (see T_m^{onset}, T_c^{onset}, T_m^{frict}, T_c^{frict} in Table 2). This effect is in line with two observations which have a particular impact on the latter emulsion. Firstly, it is consistent with the idea that the protective barrier formed by silicone oil and surfactant slows down the process of crystallisation and melting. Secondly, a similar trend of reduced phase change temperatures and enthalpies was found in multiple thermal reliability studies on stearic acid after intense processing, which is the case for tribological testing [52,53]. On the other hand, as it is well known, the effect of shear/friction can significantly disturb the way crystals grow and melt, leading to changes in their thermal characteristics. Therefore, this result clearly indicates that the high shear rate in tribological tests exerts an evident contribution to the increase in the crystal nuclei density [54]. In addition, extra energy can be provided by this friction, which promotes both crystallisation and melting mechanisms and modifies their thermal points to early stages due to the easy particle diffusion under friction [55].

3.4. Optical microscopy

The influence of the tribological process on the crystal's formation in PCMLEs was also studied by optical microscopy analysis. Micromorphology images were taken at room temperature over the fresh samples and upon application of tribological-temperature heating–cooling ramp tests on PMMA plates. Thus, Fig. 10 shows the optical images with/without cross-polarised light for the three PCMLEs with different disperse phase concentrations, aimed at identifying the effect of friction force on the formation of crystalline structures, which can be seen as bright regions under cross-polarisers. Albeit the influence of the stearic acid concentration in PCMLE, detailed in a previous publication [20], the effect of friction on the crystallisation process of these emulsions was further evaluated in this research.

Firstly, according to the optical micrographs, the multiphasic nature of emulsions is revealed, with different shapes of the disperse phase that evolve from globular to needle-like or rod-like structures, depending on the disperse phase concentration. On the other hand, by inspecting the same samples under cross-polarized light in prior tribological tests (before shear), self-assembled crystalline structures are progressively developed for systems bearing PCM content above 1 wt% (SA5 and SA10). Then, this three-dimensional crystalline network is responsible for the previously reported gel-like behaviour, that would explain the observed rheological properties.

A more remarkable effect could be noted after conducting tribological tests as shown in Fig. 10. In this regard, the performance of the heating–cooling tribological temperature ramps over the formulated PCMLEs expectedly resulted in significantly lower crystallite sizes [56]. Consequently, over the course of these tribological measurements, not only liquid-to-solid phase change would likely alleviate the detrimental effect of the overheating generated in the tribological contact, but also

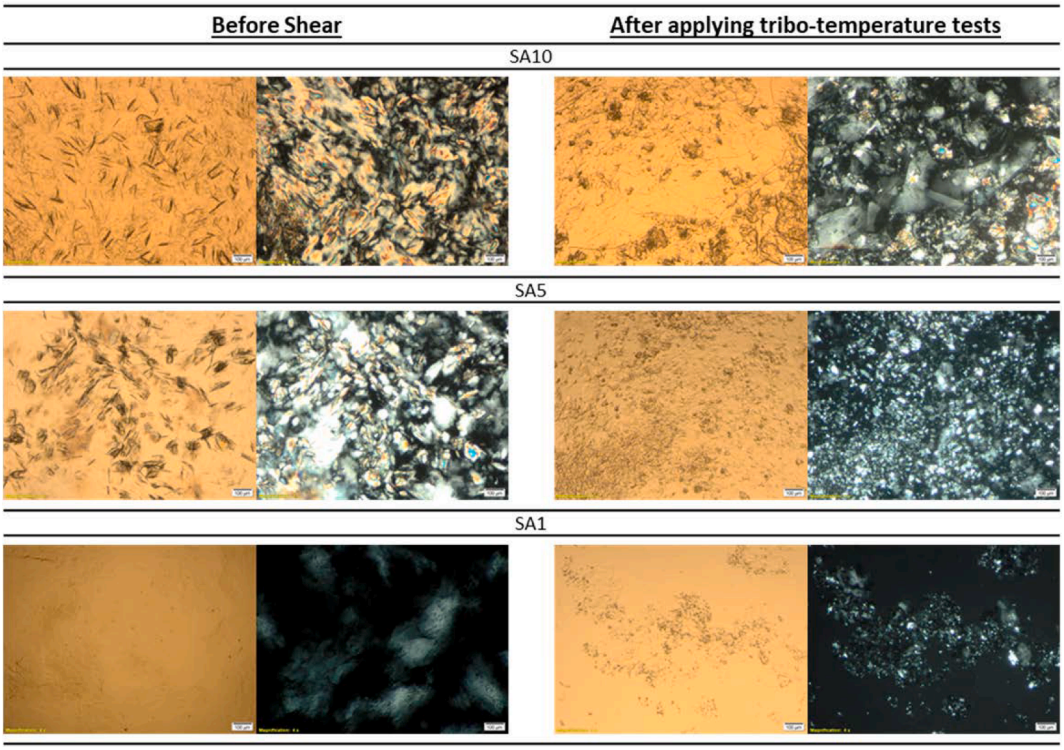

Fig. 10. Micro-morphology images of PCMLEs, at 40 °C, taken over fresh samples and after application of tribological-temperature heating–cooling ramp tests.

the crystallite breakdown may contribute to the energy dissipation process. Therefore, bearing in mind the generally lower friction coefficient and the larger tribo-film viscosity ascribed to SA10, the energy required to be dissipated throughout its tribological characterisation might be relatively lower than that corresponding to PCMLEs bearing lower stearic acid proportions, hence yielding reduced wear scar values and larger crystallites after completion of the tribological experiment (see Fig. 7). On the contrary, owing to the likely occurrence of abrasion wear during friction when considering emulsion SA1, as well as its superior frictional coefficient, an increase in the friction-generated energy within the tribological contact could be expected, resulting in smaller crystal size accordingly.

In general, it is noteworthy that, despite the high shear process endured during the friction tests, there is no observed emulsion destabilization (indicating irreversible structural changes) afterward. Instead, only a rearrangement of the microstructure is evident, underscoring the remarkable stability of lubricating emulsions.

4. Conclusions

Stable PCMLEs, composed of a dispersed stearic acid in silicone oil were successfully stabilised with an adequate non-ionic surfactant to be used as a novel lubricant with improved thermal characteristics. The reported rheological properties result in being strongly dependent on disperse phase ratio and testing temperature. Thus, at 40 °C, i.e. below the melting point of the disperse phase, stearic acid remains in a crystalline state and SAOS discloses a clear gel-like behaviour for disperse phase ratios equal to more than 5, as a consequence of the development of a three-dimensional network of crystal structures, whereas a much weaker structured network is noticed at lower ratios (SA1). However, the observed strong deviation of the empirical Cox-Merz revealed from the comparison with stationary flow tests and tribological tests pointed out a high susceptibility to shear and the weakness of the developed network, as demonstrated by optical observations. On the contrary, at 80 °C, i.e. above the melting interval of stearic acid, liquid melted droplets are dispersed in the silicone phase, leading to a low viscosity Newtonian behaviour almost independent of concentration.

The reported rheological behaviour and developed microstructure led to a remarkable improvement of the tribological characteristics since PCMLEs friction coefficients are lowered compared to silicone oil. In addition, the melting of the disperse phase also gave rise to a significant decrease in the friction coefficients. Finally, the heat storage capacity of PCMLEs contributes to the delay of the phase change temperate in the tribological temperature ramp test.

CRediT authorship contribution statement

C. Delgado-Sánchez: Writing – original draft, Investigation, Data curation, Conceptualization. **E Cortés-Triviño:** Writing – original draft, Investigation, Data curation, Conceptualization. **A. Tenorio-Alfonso:** Writing – original draft, Investigation, Data curation, Conceptualization. **F.J. Navarro:** Writing – review & editing, Investigation, Data curation, Conceptualization.

Declaration of competing interest

The authors declare that they have no known competing financial interests or personal relationships that could have appeared to influence the work reported in this paper.

Data availability

Data will be made available on request.

Acknowledgements

Grant PID2020-116905RB-I00 funded by MCIN/AEI/10.13039/501100011033 and grant TED2021-131284B-I00 funded by MCIN/AEI/10.13039/501100011033 (Spain) and European Union "NextGenerationEU"/PRTR. Clara Delgado and Adrián Tenorio also acknowledge financial support from Junta de Andalucía (Spain) through post-doctoral Grants DC 01228 (co-funded by the EU Fondo Social Europeo (FSE),

European Union) and POSTDOC_21_00644, respectively. Funding for open access charge: Universidad de Huelva / CBUA (Spain).

References

[1] S. Boyde, Green lubricants Environmental benefits and impacts of lubrication, Green Chem. 4 (2002) 293–307, https://doi.org/10.1039/b202272a.

[2] L.R. Rudnick, Synthetics, mineral oils, and bio-based lubricants: chemistry and technology, CRC Press, 2020.

[3] Y. Wu, T. Sun, Z. He, X. Zeng, T. Ren, E. de Vries, E. van der Heide, Study on the relationship between the tribological properties and oxidation degree of graphene derivatives in O/W emulsion, Tribol Int 157 (2021) 106875, https://doi.org/10.1016/j.triboint.2021.106875.

[4] A. Azushima, S. Inagaki, H. Ohta, Plating out oil film thickness on roll and workpiece during cold rolling with O/W emulsion, Tribol. Trans. 54 (2011) 275–281, https://doi.org/10.1080/10402004.2010.542275.

[5] B. Hajshirmohammadi, M.R. Forouzan, A. Heidari, Effect of interstand tensions on lubrication regime in cold strip rolling with O/W emulsion, Tribol. Trans. 62 (2019) 548–556, https://doi.org/10.1080/10402004.2018.1536238.

[6] L. Ma, C. Zhang, J. Luo, Investigation of the film formation mechanism of oil-in-water (O/W) emulsions, Soft Matter 7 (2011) 4207–4213, https://doi.org/10.1039/C0SM01561J.

[7] N. Fujita, Y. Kimura, K. Kobayashi, Y. Amanuma, Y. Sodani, Estimation model of plate-out oil film in high-speed tandem cold rolling, J Mater Process Technol 219 (2015) 295–302, https://doi.org/10.1016/j.jmatprotec.2015.01.002.

[8] A.K.L. Oppermann, L.C. Verkaaik, M. Stieger, E. Scholten, Influence of double (w 1 /o/w 2) emulsion composition on lubrication properties, Food Funct 8 (2017) 522–532, https://doi.org/10.1039/C6FO01523A.

[9] R. Taheri, B. Kosasih, H. Zhu, A.K. Tieu, Surface film adsorption and lubricity of soybean oil in-water emulsion and triblock copolymer aqueous solution: A comparative study, Lubricants 5 (2016) 1, https://doi.org/10.3390/lubricants5010001.

[10] R. Taheri, B. Kosasih, H. Zhu, TiO2–SiO2 nanoparticle-stabilized soybean oil-in-water emulsions: dispersion stability, Rolling Lubrication Performance, and Surface Self-Cleaning Effects, J Tribol 144 (2022) 1–19, https://doi.org/10.1115/1.4053356.

[11] I. Mattsby-Baltzer, M. Sandin, B. Ahlström, S. Allenmark, M. Edebo, E. Falsen, K. Pedersen, N. Rodin, R.A. Thompson, L. Edebo, Microbial growth and accumulation in industrial metal-working fluids, Appl Environ Microbiol 55 (1989) 2681–2689, https://doi.org/10.1128/aem.55.10.2681-2689.1989.

[12] H. Pivnick, W.E. Engelhard, T.L. Thompson, The growth of pathogenic bacteria in soluble oil emulsions, Appl Microbiol 2 (1954) 140–142, https://doi.org/10.1128/am.2.3.140-142.1954.

[13] K.R. Januszkiewicz, A.R. Riahi, S. Barakat, High temperature tribological behaviour of lubricating emulsions, Wear 256 (2004) 1050–1061, https://doi.org/10.1016/j.wear.2003.06.001.

[14] T.R. Forbus, Oil-in-oil emulsion lubricants for enhanced lubrication, US6972275B2, 2005.

[15] M. Shamshiri, R. Jafari, G. Momen, A novel hybrid anti-icing surface combining an aqueous self-lubricating coating and phase-change materials, Prog Org Coat 177 (2023) 107414, https://doi.org/10.1016/j.porgcoat.2023.107414.

[16] T. Xiang, J. Liu, Q. Liu, F. Wei, Z. Lv, Y. Yang, L. Ping Shi, C. Li, D. Chen, G. Xu, Self-healing solid slippery surface with porous structure and enhanced corrosion resistance, Chemical Engineering Journal 417 (2021) 128083, https://doi.org/10.1016/j.cej.2020.128083.

[17] K. Du, J. Calautit, Z. Wang, Y. Wu, H. Liu, A review of the applications of phase change materials in cooling, heating and power generation in different temperature ranges, Appl Energy 220 (2018) 242–273, https://doi.org/10.1016/j.apenergy.2018.03.005.

[18] H. Ruan, Y. Zhang, Q. Wang, C. Wang, T. Wang, A novel earthworm-inspired smart lubrication material with self-healing function, Tribol Int 165 (2022) 107303, https://doi.org/10.1016/j.triboint.2021.107303.

[19] F. Wang, W. Lin, Z. Ling, X. Fang, A comprehensive review on phase change material emulsions: Fabrication, characteristics, and heat transfer performance, Sol. Energy Mater. Sol. Cells 191 (2019) 218–234, https://doi.org/10.1016/j.solmat.2018.11.016.

[20] C. Delgado-Sánchez, A.A. Cuadri, F.J. Navarro, P. Partal, Formulation and processing of novel non-aqueous polyethylene glycol-in-silicone oil (o/o) phase change emulsions, Sol. Energy Mater. Sol. Cells 221 (2021), https://doi.org/10.1016/j.solmat.2020.110898.

[21] C. Delgado-Sánchez, P. Partal, M.J. Martín-Alfonso, F.J. Navarro, Oil-in-Oil emulsions of stearic acid dispersed in silicone oil with enhanced energy storage capability for heat transfer fluids, Sol. Energy Mater. Sol. Cells 245 (2022), https://doi.org/10.1016/j.solmat.2022.111893.

[22] N. Singh, S.K. Sinha, Tribological and mechanical analysis of hybrid epoxy based polymer composites with different in situ liquid lubricants (silicone oil, PAO and SN150 base oil), Wear 504–505 (2022) 204404, https://doi.org/10.1016/j.wear.2022.204404.

[23] E. Sneha, R.B. Akhil, A. Krishna, S. Rani, S.A. Kumar, Formulation of bio-lubricant based on modified rice bran oil with stearic acid as an anti-wear additive, Proceedings of the Institution of Mechanical Engineers, Part j: Journal of Engineering Tribology. 235 (2021) 1950–1957, https://doi.org/10.1177/1350650120977381.

[24] P. Heyer, J. Läuger, Correlation between friction and fl ow of lubricating greases in a new tribometer device, Lubr. Sci. 21 (2009) 253–268, https://doi.org/10.1002/ls.

[25] B. Wu, W. Fu, B. Kong, K. Hu, C. Zhou, J. Lei, Preparation and characterization of stearic acid/polyurethane composites as dual phase change material for thermal energy storage, J Therm Anal Calorim 132 (2018) 907–917, https://doi.org/10.1007/s10973-018-6977-5.

[26] V. Malta, G. Celotti, R. Zannetti, A.F. Martelli, Crystal structure of the C form of stearic acid, J. Chem. Soc. B (1971) 548–553, https://doi.org/10.1039/J29710000548.

[27] Y. Chen, X. Zhang, B. Wang, M. Lv, Y. Zhu, J. Gao, Fabrication and characterization of novel shape-stabilized stearic acid composite phase change materials with tannic-acid-templated mesoporous silica nanoparticles for thermal energy storage, RSC Adv 7 (2017) 15625–15631, https://doi.org/10.1039/c7ra00964j.

[28] M. Fang, C. Wu, Z. Yang, T. Wang, Y. Xia, J. Li, ZIF-8/PDMS mixed matrix membranes for propane/nitrogen mixture separation: Experimental result and permeation model validation, J Memb Sci 474 (2015) 103–113, https://doi.org/10.1016/j.memsci.2014.09.040.

[29] P. Ferreira, Á. Carvalho, T.R. Correia, B.P. Antunes, I.J. Correia, P. Alves, Functionalization of polydimethylsiloxane membranes to be used in the production of voice prostheses, Sci Technol Adv Mater 14 (2013), https://doi.org/10.1088/1468-6996/14/5/055006.

[30] K. Uvanesh, S.S. Sagiri, K. Senthilguru, K. Pramanik, I. Banerjee, A. Anis, S.M. Al-Zahrani, K. Pal, Effect of span 60 on the microstructure, crystallization kinetics, and mechanical properties of stearic acid oleogels: An in-depth analysis, J Food Sci 81 (2016) E380–E387, https://doi.org/10.1111/1750-3841.13170.

[31] L.G. Torres, R. Iturbe, M.J. Snowden, B.Z. Chowdhry, S.A. Leharne, Preparation of o/w emulsions stabilized by solid particles and their characterization by oscillatory rheology, Colloids Surf A Physicochem Eng Asp 302 (2007) 439–448, https://doi.org/10.1016/j.colsurfa.2007.03.009.

[32] M. Minale, R. Martone, C. Carotenuto, Microstructural changes of concentrated Newtonian suspensions in the first oscillation cycles probed with linear and non-linear rheology, Soft Matter 18 (2022) 6051–6065, https://doi.org/10.1039/d2sm00600f.

[33] W.P. Cox, E.H. Merz, Correlation of dynamic and steady flow viscosities, J. Polym. Sci. 28 (1958) 619–622, https://doi.org/10.1002/POL.1958.1202811812.

[34] P.E.D. Augusto, A. Ibarz, M. Cristianini, Effect of high pressure homogenization (HPH) on the rheological properties of tomato juice: Creep and recovery behaviours, Food Res. Int. 54 (2013) 169–176, https://doi.org/10.1016/j.foodres.2013.06.027.

[35] C. Carotenuto, G. Rexha, R. Martone, M. Minale, The microstructural change causing the failure of the Cox-Merz rule in Newtonian suspensions: experiments and simulations, Rheol Acta 60 (2021) 309–325, https://doi.org/10.1007/s00397-021-01270-8.

[36] B.E. Meza, A.K.S. Chesterton, R.A. Verdini, A.C. Rubiolo, P.A. Sadd, G. D. Moggridge, D.I. Wilson, Rheological characterisation of cake batters generated by planetary mixing: Comparison between untreated and heat-treated wheat flours, J Food Eng 104 (2011) 592–602, https://doi.org/10.1016/j.jfoodeng.2011.01.022.

[37] K. Manoi, S.S.H. Rizvi, Emulsification mechanisms and characterizations of cold, gel-like emulsions produced from texturized whey protein concentrate, Food Hydrocoll 23 (2009) 1837–1847, https://doi.org/10.1016/j.foodhyd.2009.02.011.

[38] G. Katsaros, M. Tsoukala, M. Giannoglou, P. Taoukis, Effect of storage on the rheological and viscoelastic properties of mayonnaise emulsions of different oil droplet size, Heliyon 6 (2020) e05788.

[39] G. Gu, Z. Wu, Z. Zhang, F. Qing, Tribological properties of fluorine-containing additives of silicone oil, Tribol Int 42 (2009) 397–402, https://doi.org/10.1016/j.triboint.2008.07.012.

[40] Z.A. Wang, Z.R. Zhou, An investigation of fretting behaviour of several synthetic base oils, Wear 267 (2009) 1399–1404, https://doi.org/10.1016/j.wear.2008.12.092.

[41] V.N. Chaudhari, M.K. Rathod, K.A. Chaudhari, Stearic acid as phase change material: thermal reliability test and compatibility with some construction materials, International Journal of Engineering Research & Technology 2 (2013) 1–8.

[42] Q. Wang, Y. Zhu, Z. Ji, J. Chen, Lubrication and sensory properties of emulsion systems and effects of droplet size distribution, Foods 10 (2021) 3024, https://doi.org/10.3390/foods10123024.

[43] H.X. Yu, X. Yu, S. Chen, J. Hao, L. Xu, A monosurfactant-stabilized dual-responsive and versatile emulsion lubricant, J Clean Prod 406 (2023) 137089, https://doi.org/10.1016/J.JCLEPRO.2023.137089.

[44] B.K. Paswan, R. Jain, S.K. Sharma, V. Mahto, V.P. Sharma, Development of Jatropha oil-in-water emulsion drilling mud system, J Pet Sci Eng 144 (2016) 10–18, https://doi.org/10.1016/J.PETROL.2016.03.002.

[45] G.E. Yakubov, T.E. Branfield, J.H.H. Bongaerts, J.R. Stokes, Tribology of particle suspensions in rolling-sliding soft contacts, Biotribology 3 (2015) 1–10, https://doi.org/10.1016/J.BIOTRI.2015.09.003.

[46] M. Masen, P. Cann, Tribology test design for friction measurements with application to oral medicines, Biotribology 35–36 (2023) 100260, https://doi.org/10.1016/J.BIOTRI.2023.100260.

[47] M.J. Palimi, V. Alvarez, E. Kuru, W.G. Chen, D.Y. Li, Effects of sliding speed on corrosion and tribo-corrosion of carbon steel in emulsion-based drilling fluids with green corrosion inhibitors, J Bio Tribocorros 9 (2023) 1–19, https://doi.org/10.1007/s40735-022-00722-9.

[48] Z. Hu, H. Zhang, H. Zhao, D. Wang, The friction and wear behavior of silicon oil-based magnetorheological fluid with solid lubricant, J Phys Conf Ser 2174 (2022), https://doi.org/10.1088/1742-6596/2174/1/012029.
[49] B. Tormos, L. Ramírez, J. Johansson, M. Björling, R. Larsson, Fuel consumption and friction benefits of low viscosity engine oils for heavy duty applications, Tribol Int 110 (2017) 23–34, https://doi.org/10.1016/j.triboint.2017.02.007.
[50] C.H. Chan, S.W. Tang, N.K. Mohd, W.H. Lim, S.K. Yeong, Z. Idris, Tribological behavior of biolubricant base stocks and additives, Renew. Sustain. Energy Rev. 93 (2018) 145–157, https://doi.org/10.1016/j.rser.2018.05.024.
[51] A.R. Lansdown. Lubrication, a practical guide to lubricant selection, Pergamon Press, Oxford, 1982.
[52] A. Sari, Thermal reliability test of some fatty acids as PCMs used for solar thermal latent heat storage applications, Energy Convers Manag 44 (2003) 2277–2287, https://doi.org/10.1016/S0196-8904(02)00251-0.
[53] A. Sari, A. Biçer, Ö. Lafçi, M. Ceylan, Galactitol hexa stearate and galactitol hexa palmitate as novel solid-liquid phase change materials for thermal energy storage, Sol. Energy 85 (2011) 2061–2071, https://doi.org/10.1016/j.solener.2011.05.014.
[54] K. Jariyavidyanont, S. Mallardo, P. Cerruti, M.L. Di Lorenzo, R. Boldt, A. M. Rhoades, R. Androsch, Shear-induced crystallization of polyamide 11, Rheol Acta 60 (2021) 231–240, https://doi.org/10.1007/s00397-021-01264-6.
[55] N. Koumakis, A.B. Schofield, G. Petekidis, Effects of shear induced crystallization on the rheology and ageing of hard sphere glasses, Soft Matter 4 (2008) 2008–2018, https://doi.org/10.1039/b805171b.
[56] B. Radel, M. Gleiß, H. Nirschl, Crystal Breakage Due to Combined Normal and Shear Loading, Crystals (basel) 12 (2022), https://doi.org/10.3390/cryst12050644.